Nucleation probability in binary heterogeneous nucleation of water–*n*-propanol vapor mixtures on insoluble and soluble nanoparticles

P. E. Wagner, D. Kaller,* and A. Vrtala
Institut für Experimentalphysik, Universität Wien, Boltzmanngasse 5, A-1090 Wien, Austria

A. Lauri and M. Kulmala
Department of Physical Sciences, University of Helsinki, P.O. Box 64, FIN-00014 Helsinki, Finland

A. Laaksonen
Department of Applied Physics, University of Kuopio, P.O. Box 1627, FIN-70211 Kuopio, Finland
(Received 5 April 2002; published 24 February 2003)

Nucleation probabilities for binary heterogeneous nucleation have been measured quantitatively. Heterogeneous nucleation of binary *n*-propanol–water vapor mixtures on partially soluble 6.9-nm NaCl particles and on nonsoluble oxidized and nonoxidized 8-nm Ag particles at a constant nucleation temperature of 288 K (NaCl) or 285 K (Ag) has been investigated experimentally and theoretically. An expansion chamber was applied to generate supersaturated vapor mixtures. Number concentrations of particles activated to condensational growth were determined optically for various vapor phase activities at constant temperature. Nucleation probabilities have been measured as functions of the vapor phase activities for several *n*-propanol–water vapor mixing ratios. Beyond certain vapor phase activities a sharp onset of heterogeneous nucleation was observed both for NaCl and for Ag particles. For insoluble particle surfaces the theoretical slopes of the nucleation probability versus vapor phase activity curves were found to be somewhat steeper as compared to the experiment. On the other hand, for soluble particles the experimental slopes were found to be in satisfactory agreement with theory. The onset of the nucleation process is defined at an activity value where 50% of the particles were activated to condensational growth. Onset activities were obtained for various mixing ratios of the binary vapor mixtures. In the case of NaCl nuclei for *n*-propanol rich mixtures, the heterogeneous nucleation calculations based on a thermodynamically consistent version of Fletcher theory and an experimentally determined contact angle provide a reasonable approximation of the experimental data. However, it appears that the Fletcher theory is not applicable in the region of transition from *n*-propanol rich to water rich mixtures. Based on the Köhler theory of activation of soluble particles, a theory was formulated accounting for the presence of two condensable vapors and limited solubility of NaCl in water-propanol liquid mixtures. This approach provides a satisfactory description of the transition from activation of soluble particles to nucleation of vapors on insoluble particles. In the case of silver particles Fletcher theory with macroscopic experimental contact angles as well as with contact angle zero results in strong deviations from experimental data. A significant improvement was achieved by introducing fit contact angles, which are substantially lower than the macroscopic experimental values and may be considered as approximate values of the microscopic contact angles.

DOI: 10.1103/PhysRevE.67.021605 PACS number(s): 64.60.Qb, 82.60.Nh

I. INTRODUCTION

Atmospheric clouds represent an everyday demonstration of heterogeneous nucleation initiated by soluble nuclei, mostly salt particles that have deliquesced at relative humidities below 100%. Another type of heterogeneous nucleation occurs on insoluble nuclei: supersaturated vapor forms liquid embryos on particle surfaces, triggering the growth of liquid droplets. More than one molecular species often participate in vapor-liquid nucleation, due to the depression of the individual equilibrium vapor pressures above liquid mixture surfaces.

Formation of atmospheric aerosols has recently received growing experimental and theoretical interest due to climate and health related effects of fine particles [1,2]. Although new theories have been developed (see, e.g., Laaksonen *et al.*, 1995 [3]), including molecular dynamics (e.g., Arstila *et al.*, 1998 [4]) and Monte Carlo simulations [5], the classical nucleation theory (see, e.g., Seinfeld and Pandis, 1998 [6]) is the only one that is practical for atmospheric applications, and particularly in atmospheric models. The classical nucleation theory requires detailed representations of various thermodynamic parameters as input [7,8]. However, laboratory experiments and also molecular approaches are needed to confirm the results obtained by classical theories and in the future, parametrized versions of molecular models can hopefully be used in atmospheric models.

Condensational growth of insoluble aerosol particles is often initiated by heterogeneous nucleation on the surface of these particles. The classical theory of heterogeneous nucleation was developed by Fletcher (1958) [9]. The theory was extended to binary systems using the capillarity approximation by Lazaridis *et al.* (1991) [10]. Heterogeneous nucleation on insoluble particles initiates changes in particle size and composition distributions, but does not increase particle

*Formerly Petersen.

 ©2003 The American Physical Society

number concentration. Soluble aerosol particles may grow as a result of equilibrium uptake of vapors (mostly water), but only when the vapor becomes supersaturated can significant mass transfer in the form of condensation take place between the phases.

While homogeneous nucleation has been studied for various unary as well as binary vapor systems, the few quantitative experiments on heterogeneous nucleation reported so far (e.g., Refs. [11–17]), are mainly restricted to unary vapors.

Kotzick *et al.* [11] investigated the heterogeneous nucleation of water vapor on soot particles applying a Nolan-Pollak counter. A reaction of soot particles with ozone [39] facilitates the heterogeneous nucleation behavior of water vapor. This is reflected in a decrease of the critical supersaturation. A Fourier transform infrared spectroscopy was applied to investigate the functional groups on the surface of a particle. Surprisingly, a significant difference between infrared spectra of the ozone treated and nontreated aerosol was not found. The untreated soot sample already revealed a significant amount of oxygen despite the aerosol generation in an Ar atmosphere.

Kotzick *et al.* [12] studied the possibility for an initially hydrophobic aerosol to act as cloud condensation nuclei by turning more hydrophilic either due to coagulation with hydrophilic particles or changing the particles' surface properties due to oxidation with ozone. Heterogeneous nucleation of water vapor on carbon particles, benzo[a]pyrene-tagged [40] carbon particles, and external mixtures of carbon particles with sodium chloride and sulfuric acid aerosols was compared. Carboneous particles were found to be able to be activated to condensational growth at atmospheric conditions after undergoing processes mentioned above.

Chen *et al.* [13] investigated the condensation of water vapor on submicrometer particles SiO_2 and TiO_2 applying a flow cloud chamber. Critical supersaturations are smaller than Fletcher theory predicts for perfectly wettable particles, even though SiO_2 and TiO_2 are insoluble in water. The discrepancy cannot be explained by the effects of line tension or surface diffusion. Further, Chen *et al.* [14] observed a similar behavior with *n*-butanol vapor and SiO_2 and TiO_2. Both aerosols induce the heterogeneous nucleation better than is predicted for perfectly wettable particles by Fletcher theory [9]. Also, lactose and monosodium glutamate particles [15] induce the heterogeneous nucleation of *n*-butanol better than particles perfectly wettable by *n*-butanol.

Oatis *et al.* [16] investigated the deliquescence and efflorescence of ammonium sulfate $(NH_4)_2SO_4$ in the presence of only partially soluble salts, $CaCO_3$ or $BaSO_4$, by means of a single particle levitation technique. While the deliquescence point of pure $(NH_4)_2SO_4$ is not influenced by the presence of $CaCO_3$ or $BaSO_4$, the influence is remarkable at the efflorescence point: this was observed at higher relative humidities while solid $CaCO_3$ or $BaSO_4$ was present in the solution of $(NH_4)_2SO_4$ and water. The shape of the deliquescence curve is also slightly different in cases with and without insoluble substances.

Han *et al.* [17] found an increase in the relative humidity at the efflorescence of $(NH_4)_2SO_4$-water solution in the presence of insoluble metal oxides Al_2O_3, ZrO_2, and TiO_2. Fourier transform infrared spectroscopy was applied to observe the efflorescence with decreasing relative humidity.

Porstendörfer *et al.* [18] investigated heterogeneous nucleation of water vapor on NaCl particles and nonoxidized Ag particles of different particle sizes applying a size analyzing nuclei counter. For Ag particles a satisfactory agreement with Fletcher theory for a contact angle 36.8° was observed. Experiments based on a similar experimental method are the focus of the investigations described in the subsequent sections.

The quantification of heterogeneous nucleation is even more difficult than that of homogeneous nucleation. This is due to the complexity of interactions between the nucleating molecules and the underlying surface. Heterogeneous nucleation rate is strongly dependent on the characteristics of the surface, and it is extremely difficult to produce well-defined surfaces for experimental investigations. The lack of experimental data, on the other hand, has made it difficult so far to verify any theoretical ideas. It seems probable that in the future further information on the details of heterogeneous nucleation phenomena will be acquired through molecular dynamics or Monte Carlo simulations [19].

In this paper the binary heterogeneous nucleation of water–*n*-propanol vapors on Ag and NaCl particles is studied. The quantitative experiments are described in Sec. II, the theoretical approaches in Sec. III, and the experimental and modeling results are given in Sec. IV.

II. EXPERIMENTS

We have performed an experimental study of heterogeneous nucleation of supersaturated binary *n*-propanol–water vapor mixtures on monodispersed Ag and NaCl particles under well defined thermodynamic conditions. For the vapor compounds selected, all physicochemical parameters required are known with sufficient accuracy. Contact angles with respect to a macroscopic Ag surface were measured for liquid mixtures with various mixing ratios [20] using the Wilhelmy plate method and a goniometer. The contact angle for *n*-propanol liquid on a NaCl surface was found to be 0° [20].

In the following we summarize the main features of the experiment; details of the experimental system are presented elsewhere [21,22]. A schematic diagram of the experimental arrangement is shown in Fig. 1. Ag or NaCl particles were generated in a high-temperature tube furnace at temperatures of about 1310 K (Ag particles) or 920 K (NaCl particles). Carefully filtered and dried air was passed through the furnace tube at constant flow rate. Ag or NaCl was evaporated from a ceramic boat and subsequent cooling resulted in homogeneous nucleation of particles. For the case of Ag particles, alternatively, air or high-purity nitrogen was used to study possible effects of oxidation. A monodispersed fraction of the aerosol with an average diameter of approximately 8 nm was extracted by means of an electrostatic aerosol classifier and subsequently neutralized. The size distribution of this aerosol fraction was measured using a differential electrical mobility spectrometer (EMS) and geometric standard

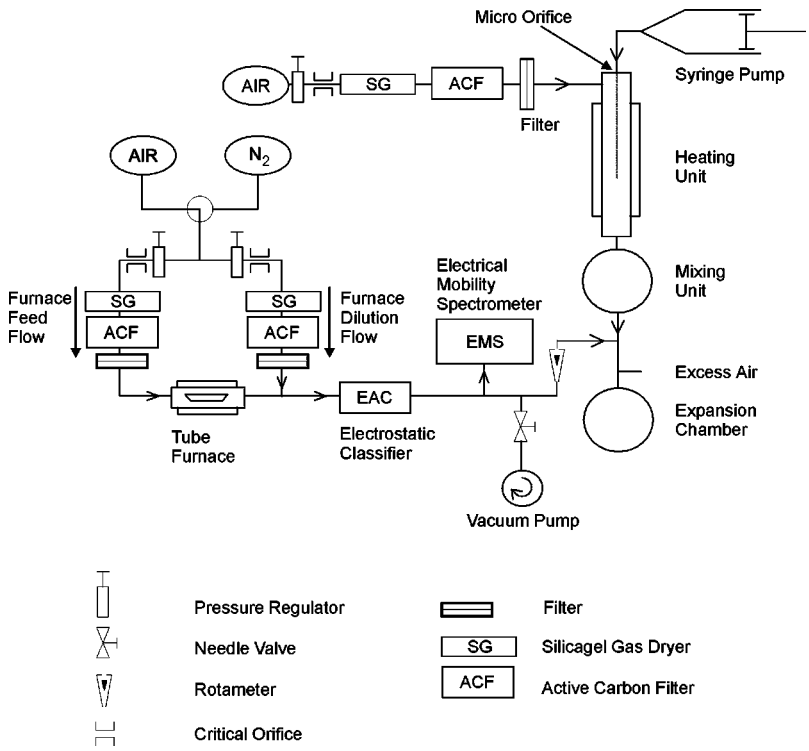

FIG. 1. A schematic diagram of the experimental system.

deviations of 1.07 (Ag particles) and 1.05 (NaCl particles) were found.

It is well known that NaCl particles produced by the method we employ are aggregates of smaller primary particles, which can be made to collapse to denser structures, for example, due to cohesive forces between adsorbed vapor molecules [23]. We tested this possibility by introducing the 8-nm NaCl particles to saturated propanol vapor. The resulting particle size was 6.9 nm, which we employed in the calculations described below. Similar experiments with subsaturated water vapor have shown that the reduction of NaCl particle size is practically independent of the solubility of the particle compound in the condensing liquid.

Binary *n*-propanol–water vapor mixtures in air were obtained by means of the spray-evaporation method. A liquid mixture with the desired mixing ratio was injected by a high-precision syringe pump through a micro-orifice with a diameter of 20 μm into a heating unit at a selectable, constant feed rate. The resulting liquid beam was quantitatively evaporated and mixed with carefully filtered and dried air as well as with the monodispersed aerosol at flow rates precisely controlled by means of critical orifices. Homogeneous mixtures of air, *n*-propanol, and water vapor were obtained in a mixing unit. It should be emphasized that the partial vapor pressures obtained are defined by the compositions of the liquid mixture and the flow rates considered without reference to literature data on equilibrium vapor pressures. In order to achieve the desired vapor supersaturations, the binary vapor mixtures obtained together with the aerosol considered were passed into a thermostated expansion chamber. During a computer controlled measurement cycle adiabatic expansion was initiated by opening of a valve connecting the chamber to a low-pressure buffer tank. The pressure drop inside the expansion chamber was monitored by a fast precision pressure transducer. Expansion times around 5 ms were typically observed. Temperature and vapor phase activities after expansion were determined using Poisson's law. It is notable that the buffer tank will prevent any significant changes of the total gas pressure in the chamber after expansion has occurred.

Those particles causing heterogeneous nucleation at the vapor phase activities considered will grow to visible sizes. Size and number concentration of the growing drops were measured by means of the constant-angle Mie scattering method [24]. To this end the growing particles in the expansion chamber are illuminated by a laser beam. The light flux scattered at a selectable, constant scattering angle, as well as the light flux transmitted through the expansion chamber, are monitored by appropriate sensors, which have been calibrated relative to each other. In order to compensate for possible influences of extinction on the scattered light flux, it is normalized relative to the light flux transmitted through the expansion chamber. The normalized scattered light flux vs time curves obtained show a quite rich morphology in quantitative agreement with corresponding theoretical light flux vs size curves calculated according to Mie theory. After establishing a unique correspondence between experimental and theoretical light scattering extrema, size and number concentration of the growing droplets can be determined independently and quantitatively without referring to any external empirical calibration.

Before performing experiments on heterogeneous nucleation, the actual unary vapor phase activities occurring after the adiabatic expansion were verified by comparing experimental and theoretical drop growth curves [25]. In fact, drop growth rate is a very sensitive indicator for vapor supersaturations. Based on comparisons of experimental and theoretical droplet growth rates it can be estimated that possible

errors of the vapor phase activities obtained after expansion are less than $\pm 1\%$.

Heterogenous nucleation was studied during a series of subsequent measurements of the droplet concentration N at stepwise increasing vapor phase activities. Beyond certain activities, an increase of the droplet concentration was observed. Upon further increase of the vapor phase activities the droplet concentration was found to approach a constant value, N_{tot}, indicating that all particles were finally activated. Correspondingly, the heterogenous nucleation probabilities, $P=N/N_{tot}$, can be obtained experimentally. A quite steep increase of the nucleation probabilities with increasing activities can be observed. The vapor phase activities, at which $P=0.5$ and thus half of the particles are activated, will in the following be referred to as onset activities for heterogeneous nucleation.

It is notable that all data points refer to a constant nucleation temperature (285 or 288 K for measurements with Ag or NaCl particles, respectively). In order to obtain isothermal nucleation probability curves, the vapor phase activities after expansion in the expansion chamber were varied by changing the liquid feed rate from the syringe pump rather than changing the expansion ratio.

A quantitative comparison of the experimentally obtained nucleation probabilities and the corresponding onset activities with corresponding theoretical calculations will be presented and discussed below.

III. THEORY

In this work the extended classical theory of binary heterogeneous nucleation was applied to water–n-propanol mixtures (see Kulmala *et al.*, 2001 [22]). In this theory the critical embryos, although sometimes consisting only of a few molecules, are considered to be objects with macroscopic properties. The physicochemical properties needed for the calculations are surface tension, contact angle, density, saturation vapor pressures, and activities as a function of composition and temperature.

For soluble mixtures the activation theory (see also Petersen *et al.*, 2001 [26]) has been used as well.

A. Heterogeneous nucleation

1. Energy barrier

First we summarize the theory for homogeneous nucleation. Consider a binary cluster consisting of n_w molecules of species w and n_a molecules of species a suspended in supersaturated vapor where the temperature is T, the vapor pressure is P_v, and the mole fraction of species a in the vapor is x_{av}. The cluster is modeled as a uniform spherical liquid droplet of radius r and volume $V=\frac{4}{3}\pi r^3$. Let ρ_{il} be the number density of species i in the uniform liquid. The total number of molecules of species i is expressed as $n_i = n_{il}+n_{is}$, where the number of molecules in the bulk phase is $n_{il}=\rho_{il}V$, and n_{is} is the surface excess number of molecules that corrects for the difference between the density profiles of our uniform droplet model and the actual cluster. The critical cluster size (denoted by the asterisk) can be found by minimizing the formation free energy of a cluster with respect to n_a and n_w (see Laaksonen *et al.*, 1999 [27] for details). If we assume that the liquid is incompressible, we obtain the equation

$$v_a \Delta\mu_w = v_w \Delta\mu_a, \tag{1}$$

which can be used to find the composition of the critical nucleus x_{il}. Here $\Delta\mu_i=\mu_{il}(T,P_v,x_{il})-\mu_{iv}(T,P_v,x_{iv})$ with μ_{il} and μ_{iv} denoting the liquid and vapor phase chemical potentials, respectively, and $v_{il}(T,x_{il})$ is the partial molecular volume of species i.

Now we fix the position of the dividing surface determined by r^* so that it coincides with the surface of tension, which means that we require $[\partial\sigma/\partial r^*]=0$ to hold [28]. The radius of the cluster can then be obtained from the Kelvin equations

$$\Delta\mu_i + \frac{2\sigma v_i}{r^*} = 0 \quad (i=w,a). \tag{2}$$

The free energy of formation of the critical cluster is now given by

$$\Delta G^* = \frac{4}{3}\pi r^{*2}\sigma. \tag{3}$$

It has been shown [27] that the surface of tension is independent of the curvature of the droplet if (and only if) the condition

$$n_{ws}v_w + n_{as}v_a = 0 \tag{4}$$

holds at the surface of tension. In nucleation calculations, the surface tension of a flat surface is practically always used, since no other data are available. Thus, for the theory to be internally consistent, one has to assume (albeit implicitly) that the equimolar surface specified by Eq. (4) coincides with the surface of tension.

If the nucleation takes place heterogeneously, i.e., is initiated by a pre-existing particle, the theory is somewhat altered. The Gibbs free energy of formation of a critical cluster from a binary mixture of vapors onto a curved surface is given by the expression [9]

$$\Delta G^*_{Het} = \frac{1}{2}\Delta G^*_{Homo} f(m,z). \tag{5}$$

Here

$$f(m,z) = 1 + \left(\frac{1-mz}{g}\right)^3 + z^3\left[2 - 3\left(\frac{z-m}{g}\right) + \left(\frac{z-m}{g}\right)^3\right] + 3mz^2\left(\frac{z-m}{g} - 1\right) \tag{6}$$

with

$$g = (1+z^2-2mz)^{1/2} \tag{7}$$

and

$$z=\frac{R_p}{r^*}, \tag{8}$$

where R_p is the radius of curvature of the solid surface. The contact angle θ is given by $\cos\theta=m=(\sigma_{13}-\sigma_{23})/\sigma_{12}$, where σ_{ij} is the interfacial free energy between the phases i and j. The gas phase is indexed by 1, the cluster by 2, and the substrate by 3. The contact angle used in the case of water–n-propanol mixture was based on experiments [20] yielding the following result:

$$\theta=\frac{92.567\,36+388.2953x}{1+24.127\,55x}, \tag{9}$$

x being the mole fraction in the critical cluster. Equation (9) gives the value of the contact angle in degrees. The radius r^* of the critical cluster is the same as given by homogeneous nucleation theory. Thus, the heterogeneous critical cluster can be thought of as a segment of the homogeneous nucleus specified by the contact angle and the curvature of the underlying surface.

2. Nucleation rate and nucleation probability

The nucleation rate can be expressed as [29,30]

$$I=R_{av}FZ\exp\left(-\frac{\Delta G^*}{kT}\right). \tag{10}$$

Here R_{av} denotes the average condensation rate and F denotes the total number of nucleating molecules, clusters, particles, etc., depending on the system in question. (For instance, in homogeneous nucleation F would be the total number of molecules in the vapor, and in ion-induced nucleation the number of ions). In the case of heterogeneous nucleation the identification of F is not straightforward. Several different expressions for the factor F in heterogeneous nucleation rate can be found in the literature.

The heterogeneous nucleation rate includes the adsorption mechanism through the quantity N^{ads} (the total number of molecules adsorbed per unit area on the solid nuclei). The number of adsorbed water molecules is $N_w^{ads}=\beta_w\tau_w$. Here β_i is the impinging rate of molecules of species i on the surface of the solid particle and τ_i is the time that a molecule i spends on the surface of the solid particle. In the n-propanol–water mixture both water and n-propanol molecules have to be taken into account. Thus the total number of adsorbed molecules is $N^{ads}=N_w^{ads}+N_a^{ads}=\beta_w\tau_w+\beta_a\tau_a$.

The residence time is given by $\tau=\tau_o\exp(E/RT)$, where τ_o is a characteristic time and E is the heat of adsorption. For E Lazaridis *et al.* (1991) [10] used the latent heat of condensation given by Adamson (1982) [31]. Hamill *et al.* (1982) [32] used the value 2.4×10^{-16} s for τ_0, and the value 10 800 cal/mol for E, while Lazaridis *et al.* (1991) [10] made use of the fact that τ_o corresponds to $1/\nu_o$ [31], where ν_o is the characteristic frequency of vibration. The vibration between two molecules can be calculated using the nearest-neighbor harmonic oscillator approximation. The angular frequency (ω) of the oscillator is

$$\omega=2\pi\nu=\sqrt{\frac{d^2V}{dr^2}\frac{1}{m_\mu}}, \tag{11}$$

where m_μ is the reduced mass of the two molecules. For V Lazaridis *et al.* (1991) [10] used the modified Lennard-Jones potential of polar molecules resulting in $\tau_o=2.55\times10^{-13}$ s, which corresponds to water-water interaction. For n-propanol–n-propanol interaction the calculated value is $\tau_0=1.13\times10^{-12}$ s. In this study the temperature-dependent value of E was 10 640 cal/mol for water and 11 740 cal/mol for n-propanol at $T=285$ K.

The nucleation rate corresponds to the rate of parent particles activated to growth, i.e., formation of the first critical cluster on the surface of the particle [10]:

$$I_{Het}=4\pi R_p^2N^{ads}R_{av}ZN_{par}\exp\left(-\frac{\Delta G^*}{kT}\right). \tag{12}$$

Here N_{par} is the number concentration of the solid particles. The average condensation rate R_{av} is given by

$$R_{av}=\frac{A\beta_w\beta_a}{\beta_w\sin^2\theta+\beta_a\cos^2\theta}, \tag{13}$$

where A denotes the surface area of the embryo lying on the surface of a pre-existing particle and $\theta=\arctan[x/(1-x)]$, where x is the mole fraction of species a in the nucleus [30].

The probability for one particle to nucleate within some nucleation time t is

$$P=1-\exp(-I_{Het}t). \tag{14}$$

The theoretical onset activities, where half of the number of aerosol particles are activated to growth, were determined in the model runs by setting the nucleation probability to 0.5.

B. Activation theory

The nucleation of water vapor on deliquesced soluble particles (activation) can be described by the Köhler theory [33]. Köhler activation is a mechanistic rather than stochastic nucleation process since the droplet growth is not initiated by a free-energy barrier crossing at a metastable state. To understand the Köhler theory, consider the coexistence of aqueous salt droplets with humid air. The salt, which is assumed to be completely involatile, depresses the equilibrium vapor pressure of water above droplet surface (Raoult effect). On the other hand, the droplet curvature tends to increase it (Kelvin effect). By plotting the equilibrium relative humidity as a function of droplet diameter for a given amount of salt in the droplet, one obtains a so called ''Köhler curve,'' which is the result of the competition between the Raoult and the Kelvin effects. The curve exhibits a maximum (the Köhler maximum) at some relative humidity slightly above 100%. The Köhler maximum becomes higher as the diameter of the original salt particle is lowered. When the relative humidity is raised above the maximum, the solution droplet is said to activate, and the droplet starts growing rapidly due to nonequilibrium condensation of water.

When heterogeneous water-propanol nucleation takes place on NaCl particles, Köhler activation is expected to take place in water rich vapor mixtures. However, the addition of *n*-propanol into the water solution decreases the NaCl solubility very effectively. The Köhler theory has therefore to be modified. First of all, there are now two equations describing the equilibrium, one for water vapor and one for *n*-propanol vapor [34]. Second, the decreased solubility of the salt nucleus needs to be accounted for. Therefore, consider the equilibrium of a ternary *n*-propanol–water–NaCl solution droplet containing a partially dissolved salt core. At given moles of *n*-propanol and water in the droplet, the number of salt moles is obtained from solubility. The equations describing the equilibrium are

$$A_i = \frac{P_i}{P_{si}} = x_i f_i \exp\left(\frac{2\sigma v_i}{kTR}\right), \tag{15}$$

where A_i is the vapor phase activity of species i (either water or propanol), P_i is partial pressure of i, P_{si} is the saturation vapor pressure of pure species i, x_i is the mole fraction of i in the ternary solution, f_i is the activity coefficient of i, v_i is the partial molecular volume of i, and R is droplet radius, given by

$$R = \left[\frac{3}{4}\pi(V_c + n_w v_w + n_a v_a + n_s v_s)\right]^{1/3}. \tag{16}$$

Here V_c is the volume of the undissolved NaCl core, and the n's are the numbers of molecules for water, alcohol, and salt in the solution.

Because there are no experimental equations available for the activity coefficients of the water–propanol–sodium chloride system, we have to estimate them. An accurate description of the phase equilibrium of water–organic-electrolyte solutions would involve a combination of thermodynamic models such as the UNIFAC (universal functional group activity coefficient) model that describes organic solutions and the Pitzer model that describes electrolytes. However, that would be a very time consuming task, and instead we resort to a more approximate treatment by characterizing the system as pseudobinary [35]. In other words, we assume that in the solution, the salt is in ionic form and associated only with water, which permits treating the system as if composed of two components (propanol and water+salt). We can thus obtain an estimate for the water and propanol activity coefficients in the ternary system using experimental expressions for binary water-propanol and water-NaCl activity coefficients [35]. In practice, we define a new alcohol mole fraction $y = n_a/(n_a + n_w)$ and calculate Van Laar activity coefficients γ_a^{vl} and γ_w^{vl} for propanol and water, respectively, as a function of y. We then calculate the water activity coefficient γ_w^s in an aqueous NaCl solution having a water mole fraction of $z = n_w/(n_w + 2n_s)$. The propanol and water activity coefficients required for Eq. (15) are then given by $\gamma_a = \gamma_a^{vl}$ and $\gamma_w = \gamma_w^{vl}\gamma_w^s$.

In water-propanol solutions, the NaCl solubility decreases strongly and quite nonlinearly as a function of propanol concentration. The pseudobinary approximation is best suited for solutions in which the salt solubility decreases more or less linearly as the concentration of the organic compound increases. The pseudobinary approximation is therefore probably quite simplified in the water-propanol–NaCl system; however, we believe that it is still a better assumption than, e.g., ideality of the solution.

The surface tension of the ternary system is also unknown and has to be estimated. As a basis, we use the binary water-propanol surface tension calculated using the mole fraction y, and add a correction term due to the salt. The correction term is given by the difference between the surface tension of an aqueous salt solution having the mole fraction z and the surface tension of pure water.

The number of dissolved salt molecules, n_s, in a droplet with n_w water molecules and n_a propanol molecules can, in principle, be obtained from experimental solubility data. However, small particles are known to have increased solubilities compared to larger particles [36]. To account for the size effect we should know solid-liquid surface tensions, which are not available. On the other hand, using handbook solubilities results in unphysical nucleation behavior (nonmonotonously behaving onset activity curve). We therefore have to resort to using the solubility as a function of propanol concentration as an adjustable parameter. The NaCl solubility mole fraction that we apply in our calculations is given by $n_s/(n_w + n_a + n_s) = 0.0993(1-y)^{1.07}$. This leads to quite high solubilities at intermediate solution compositions compared to experimental bulk solubilities. Whether the necessity of using such a functional form for the solubility is caused by our approximate activity coefficients and surface tension, or by some physical feature missing from the theoretical formulation (such as the solubility size dependence or the disjoining pressure effect present in thin films; see, e.g., [37]), has to be left for future consideration.

When making numerical calculations with the activation theory, we look for equilibria at a fixed ratio A_a/A_w by iteratively solving Eqs. (15) for water and propanol. For a given number of water molecules in the solution (n_w) we then obtain n_a, A_w, and A_a. In the modified theory the salt core can be partially or totally dissolved. When plotting the diameter of the droplet versus water activity at fixed A_a/A_w, we obtain curves that have two maxima [26]. The first maximum is found for the completely undissolved salt particle, and the second one corresponds to the ordinary Köhler maximum. In water-rich vapor mixtures the second maximum is higher, and thus nucleation requires a water activity higher than that at the Köhler-type maximum. In propanol-rich mixtures the first maximum is higher, and thus nucleation requires activation of the dry NaCl particle, which takes place when water activity becomes higher than that at the first maximum.

Note that because the activation theory is not a probabilistic theory, in the same sense as the heterogeneous nucleation theory described in the previous sections, there is no way to obtain a nucleation probability curve for a strictly monodisperse particle size distribution. In other words, for particles of a given size the probability of activation is assumed to be zero when the vapor activities are below those of the higher of the two maxima described above, and unity when the maximum is reached. However, since the saturation

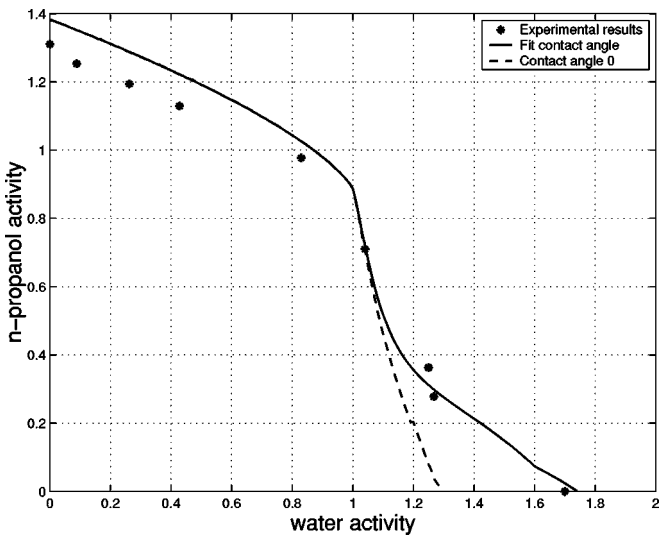

FIG. 2. Experimental onset vapor phase activities for heterogeneous nucleation of binary *n*-propanol–water vapor mixtures on Ag particles (stars). Results of corresponding model calculations based on the Fletcher approach for contact angle zero (dashed line) and for a contact angle according to a fit function (solid line) are shown.

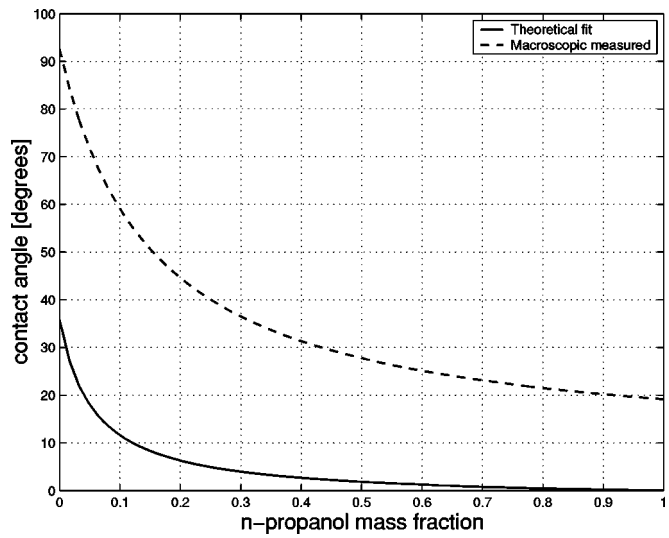

FIG. 3. Contact angle θ for binary *n*-propanol–water liquid mixtures on an Ag surface vs the *n*-propanol liquid mass fraction obtained from macroscopic measurements (dashed line) and according to a fit procedure (solid line).

ratio at the maximum depends on the size of the dry particle, a curve corresponding to the nucleation probability curve can be calculated if the dry particle size distribution is known.

IV. RESULTS AND DISCUSSION

We have measured heterogeneous nucleation probabilities for nucleation of *n*-propanol and water vapor on Ag and NaCl particles. Furthermore, heterogeneous nucleation of *n*-propanol–water vapor mixtures with various mixing ratios on Ag and NaCl particles was considered. We performed nucleation measurements for oxidized and nonoxidized Ag particles. Surprisingly, no significant differences of the nucleation behavior were observed and for the following we thus consider only the results for oxidized Ag particles. All measurements were performed at a constant nucleation temperature. From the experimental nucleation probabilities we obtained the corresponding onset activities for heterogeneous nucleation. Onset activities as well as nucleation probabilities for heterogeneous nucleation were quantitatively compared with theoretical predictions.

In Fig. 2 the experimental onset activities for heterogeneous nucleation on Ag particles (oxidized) at a constant nucleation temperature of 285 K are shown as functions of the respective vapor phase activities. For calculation of heterogeneous nucleation probabilities and onset activities according to Fletcher theory the respective contact angles are required. Contact angles for liquid *n*-propanol–water mixtures on macroscopic Ag surfaces have been measured [20], the dependence of the contact angle on the *n*-propanol liquid mass fraction is shown in Fig. 3. As can be seen, the contact angle varies between about 90° for pure water and 20° for pure *n*-propanol. Fletcher calculations based on these macroscopic contact angles result in strange behavior and severe discrepancies from experimental data, even for the pure systems, as discussed elsewhere [22]. As can be seen from Fig. 2, taking a contact angle of 0° for all liquid mass fractions leads to fair agreement with experimental data, except for water rich mixtures. Somewhat increased onset activities for nucleation of water on Ag particles have also been observed by Porstendrfer *et al.* [18]. In order to account for this apparent hydrophobic behavior of the Ag particles we assumed some increase of the contact angle with decreasing *n*-propanol liquid mass fractions up to a value of about 30° as shown in Fig. 3. Thereby satisfactory agreement of Fletcher theory and experiment can be achieved for all vapor mixing ratios considered as can be seen in Fig. 2. The two curves in Fig. 3 illustrate the differences between macroscopic and microscopic contact angles. The microscopic contact angle based on the experiments is

$$\theta = \frac{35.82(1-x)}{1+61.62x} \tag{17}$$

where x is the mole fraction of *n*-propanol in the critical cluster. Equation (17) gives the contact angle in degrees. The estimated error for vapor phase activities is ± 0.01 and for nucleation probability $\pm 6\%$. These results underline the importance of a proper characterization of the microscopic particle surface in order to allow a quantitative description of heterogeneous nucleation processes.

The onset activities for heterogeneous nucleation on NaCl particles are shown as functions of the vapor phase activities in Fig. 4. While Ag is insoluble in both water and *n*-propanol liquids, it is notable that NaCl is practically insoluble in *n*-propanol liquid, but soluble in water. Correspondingly, a different nucleation behavior is observed, as can be seen in Fig. 4. Due to the solubility of NaCl in water, the onset activities are substantially reduced for water rich mixtures. On the other hand, somewhat higher onset activities as compared to Ag particles are even observed for heterogeneous

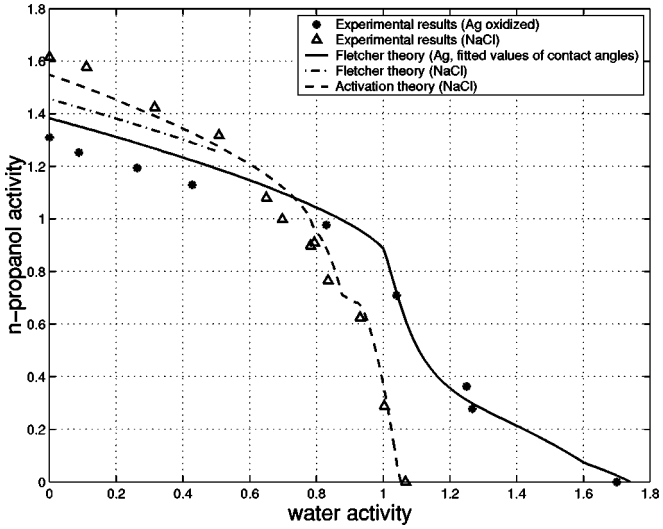

FIG. 4. Experimental onset vapor phase activities for heterogeneous nucleation of binary *n*-propanol–water vapor mixtures on Ag particles (stars) and on NaCl particles (triangles). Results of corresponding model calculations based on the Fletcher approach for Ag particles and a contact angle according to a fit function (solid line) and for NaCl particles and zero contact angle (dash-dotted line) are shown. Furthermore, onset vapor phase activities according to the activation theory for NaCl particles are indicated (dashed line).

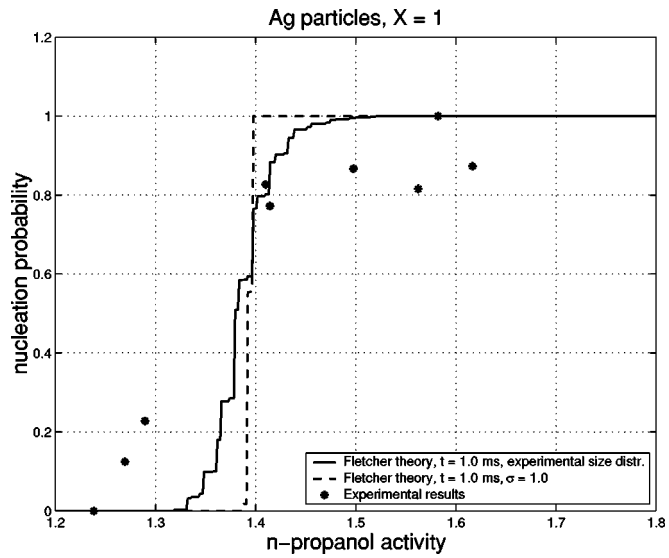

FIG. 5. Experimental heterogeneous nucleation probability for heterogeneous nucleation of binary *n*-propanol–water vapor mixtures on Ag particles vs vapor phase activity (stars). Results of corresponding model calculations based on the Fletcher approach for a contact angle according to a fit function and for experimental (solid line) as well as monodispersed (dashed line) particle size distribution are shown. *n*-propanol vapor mass fraction $X=1$, contact angle $\theta=0°$.

nucleation of *n*-propanol rich mixtures on NaCl particles, even though NaCl is completely wettable by *n*-propanol [20]. For SiO_2 and TiO_2 particles a similar effect was observed by Chen *et al.* [13].

Slightly higher onset activities are expected due to the above mentioned reduction of NaCl particle size in the presence of polar vapors. We have calculated the onset activities for nucleation of *n*-propanol rich vapor mixtures on NaCl particles according to Fletcher theory assuming a contact angle of 0° corresponding to complete wettability and accounting for the reduction of NaCl particle size. As can be seen from Fig. 4, due to the particle size reduction slightly increased onset activities are found for NaCl as compared to Ag particles, however, the experimental values for NaCl particles are still higher.

Fletcher theory is not applicable for nucleation of water rich vapor mixtures on the water soluble NaCl particles. The activation theory [Eqs. (15) and (16)], based on Köhler theory for soluble particles, on the other hand, shows rather good overall agreement with the experimental data. At water-rich vapor compositions this is an expected result, but for propanol-rich vapors it is quite remarkable that the activation theory performs similarly well as the heterogeneous nucleation theory. On the other hand, the experimental data at high propanol activities show some scatter, the nature of which remains unclear for the time being. For pure propanol, the activation theory corresponds to barrierless heterogeneous nucleation. The Fletcher theory, on the other hand, gives a finite nucleation probability in the presence of a nucleation barrier, and it therefore predicts a slightly lower onset activity than the activation theory. The soluble-insoluble transition occurring at intermediate mixing ratios has been discussed elsewhere [26].

The onset activity curves obtained in this study for heterogeneous nucleation on Ag and NaCl particles (Figs. 2 and 4) show a convex shape. Accordingly, only limited mutual enhancement of heterogeneous nucleation due to the simultaneous presence of the two vapors is observed both for Ag and NaCl particles. A much more pronounced mutual enhancement was observed for homogeneous nucleation of *n*-propanol–water vapor [38]. The heterogeneous nucleation of *n*-propanol–water vapor thus shows a qualitatively different behavior as compared to the homogeneous nucleation of *n*-propanol–water vapor.

Figures 5–8 show the nucleation probabilities for heterogeneous nucleation on Ag particles (oxidized) as functions of the vapor phase activity of one of the vapor components for various *n*-propanol–water vapor mixtures at different *n*-propanol vapor mass fractions X. The experimental data are compared with calculations based on Fletcher theory. According to the contact angle fit shown in Fig. 3, for *n*-propanol rich vapor mixtures (Figs. 5 and 6) the contact angle was taken to be 0°. For the water rich systems considered (Figs. 7 and 8) contact angles of 5.5° and 35.6°, respectively, were assumed in the calculations. The actual experimental particle size distribution, as obtained from EMS measurements, was taken into account in the Fletcher calculations. The nucleation probabilities increase with increasing vapor phase activity and certain slopes of the nucleation probability curves are observed. While the measured onset activities are described reasonably well by Fletcher theory, the slopes of the experimental nucleation probability curves are considerably smaller as compared to the Fletcher calculations. The strongest deviations of the slopes seem to occur for the one-component vapors.

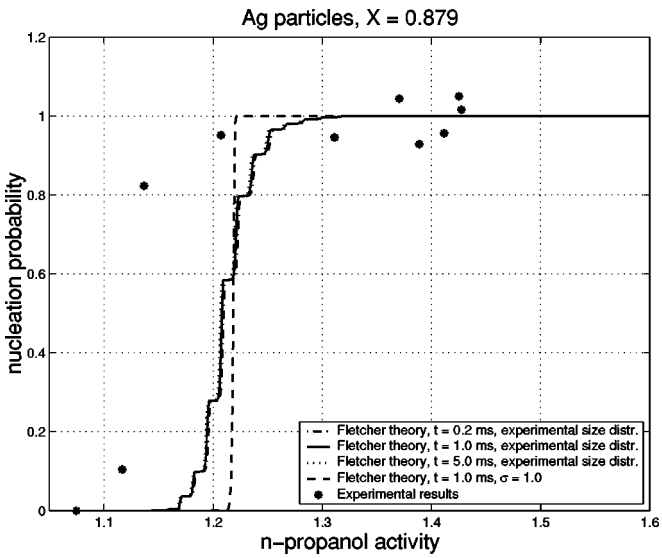

FIG. 6. Same as Fig. 5 but for *n*-propanol vapor mass fraction $X=0.879$, contact angle $\theta=0°$. In addition theoretical results for nucleation times 0.2 ms (dash-dotted line) and 5.0 ms (dotted line) are shown for comparison.

In order to study the influence of the distribution of Ag particle sizes on the nucleation probabilities, we performed nucleation calculations assuming strictly monodispersed particles as well. As can be seen from Figs. 5–8, the finite width of the Ag particle size distribution is found to have a significant influence on the heterogeneous nucleation probabilities, however, this influence is not sufficient to explain the observed deviations from experiment.

For the Fletcher calculations we used an estimated nucleation time of 1 ms. In order to investigate the influence of the nucleation time on the calculated nucleation probabilities, we considered nucleation times of 0.2 and 5 ms as well. As can be seen from Fig. 6, however, within certain limits changes of the nucleation time will cause only insignificant changes

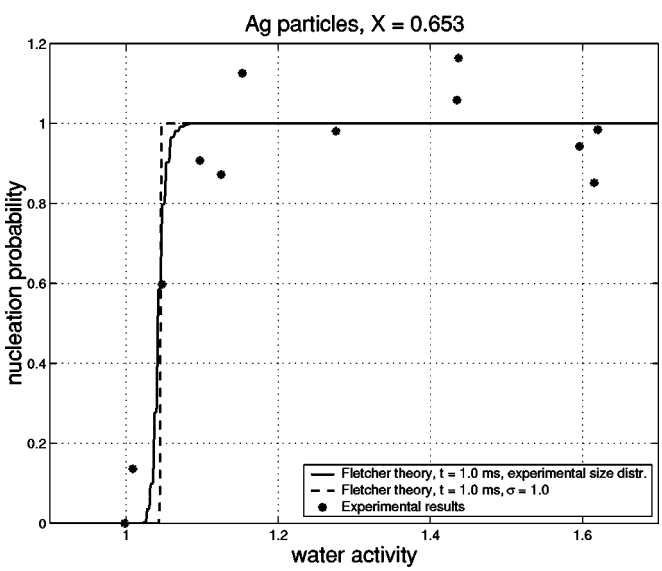

FIG. 7. Same as Fig. 5 but for *n*-propanol vapor mass fraction $X=0.653$, contact angle $\theta=5.5°$.

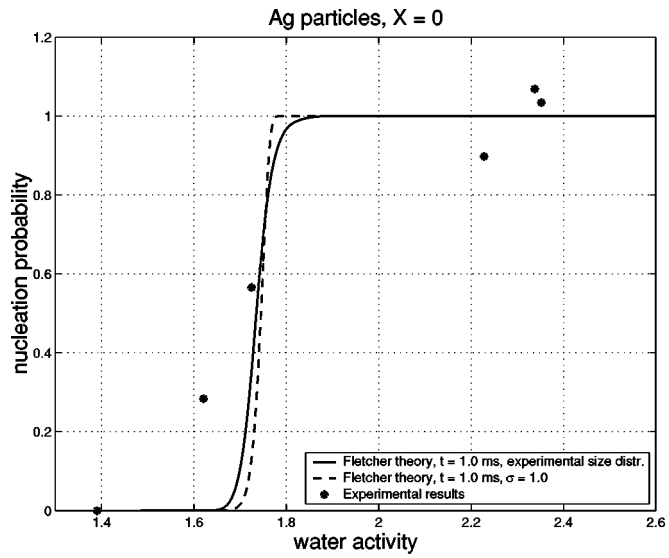

FIG. 8. Same as Fig. 5 but for *n*-propanol vapor mass fraction $X=0$, contact angle $\theta=35.6°$.

of the nucleation probabilities. The nucleation probabilities are mainly influenced by particle size, surface tension, and contact angle.

Nucleation probabilities for nucleation on NaCl particles are shown in Figs. 9–13 at different *n*-propanol vapor mass fractions *X*. The experimental data are compared with Fletcher calculations, applicable only for *n*-propanol rich vapor mixtures, and to the activation theory, which can be ap-

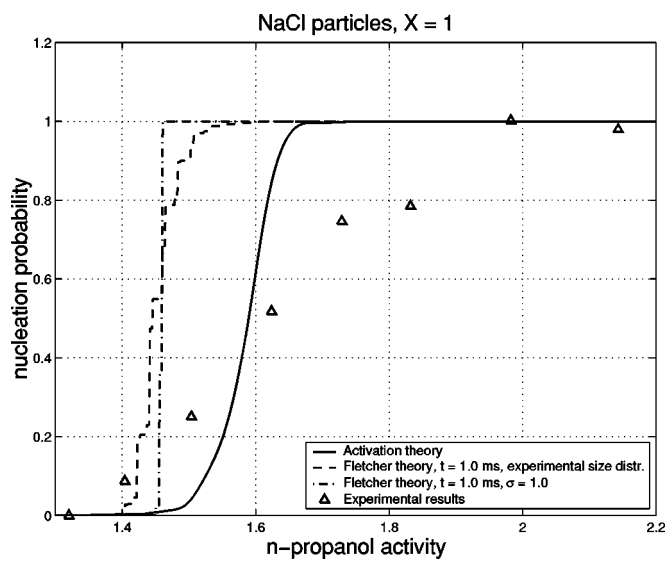

FIG. 9. Experimental heterogeneous nucleation probability for heterogeneous nucleation of binary *n*-propanol–water vapor mixtures on NaCl particles vs vapor phase activity (triangles). Results of corresponding model calculations based on the Fletcher approach for zero contact angle and for experimental (dashed line) as well as monodispersed (dash-dotted line) particle size distribution are shown. Furthermore, corresponding heterogeneous nucleation probabilities according to the activation theory for experimental particle size distribution are indicated (solid line). *n*-propanol vapor mass fraction $X=1$.

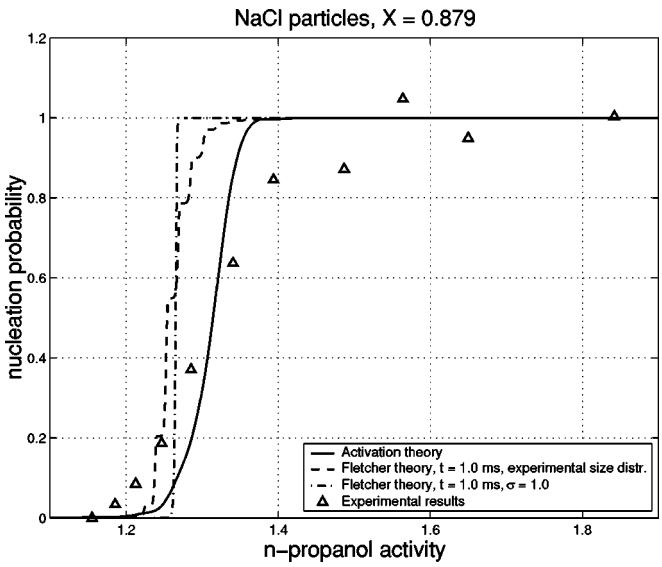

FIG. 10. Same as Fig. 9 but for *n*-propanol vapor mass fraction $X=0.879$.

plied for the entire range of vapor mixing ratios. As mentioned above, a soluble-insoluble transition occurs at a certain vapor mixing ratio having consequences for the heterogeneous nucleation probabilities. For *n*-propanol rich vapor mixtures (Figs. 9 and 10) the NaCl particles are insoluble in the condensing liquid. Correspondingly, the slopes of the experimental nucleation probability curves are significantly smaller as compared to the theoretical predictions. A similar behavior was observed for the insoluble Ag particles (see Figs. 5–8). On the other hand, for water rich vapor mixtures the NaCl particles are soluble in the condensing liquid and activation of solution droplets with well defined surface occurs. This is reflected in the considerably improved agreement of experimental and theoretical nucleation probabilities for the case of water rich vapor mixtures (Figs. 11–13). For pure water vapor as well as for water rich vapor mixtures it is observed that even the slopes of the theoretical nucleation probability curves, as calculated according to the activation theory, are in satisfactory agreement with experimental data. The activation theory is generally found to describe the heterogeneous nucleation process on NaCl particles more accurately than the Fletcher approach.

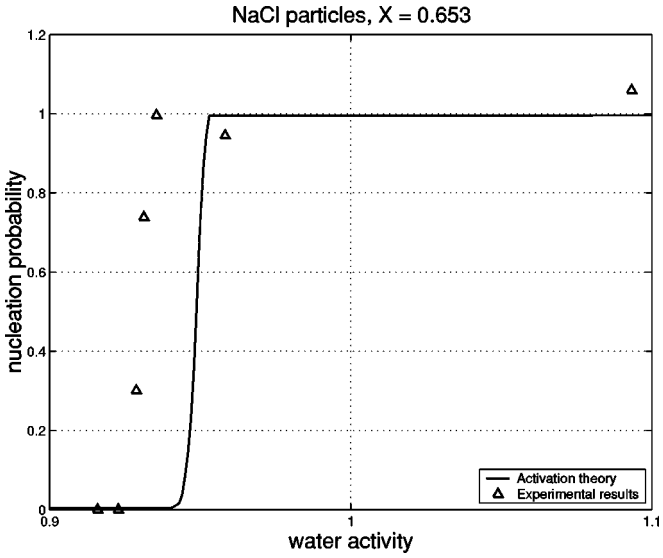

FIG. 11. Experimental heterogeneous nucleation probability for heterogeneous nucleation of binary *n*-propanol–water vapor mixtures on NaCl particles vs vapor phase activity (triangles). Corresponding heterogeneous nucleation probabilities according to the activation theory for experimental particle size distribution are indicated (solid line). *n*-propanol vapor mass fraction $X=0.653$.

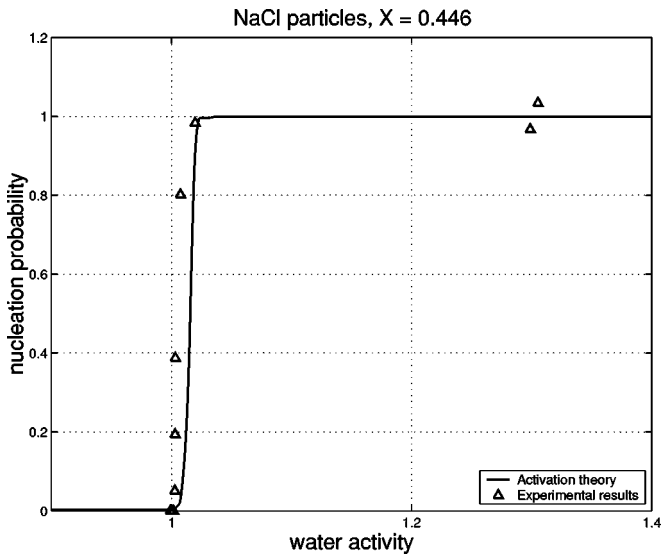

FIG. 12. Same as Fig. 11 but for *n*-propanol vapor mass fraction $X=0.446$.

V. CONCLUSIONS

Nucleation probabilities for heterogeneous nucleation of binary vapor mixtures on well defined monodispersed particles have been measured quantitatively. Heterogeneous

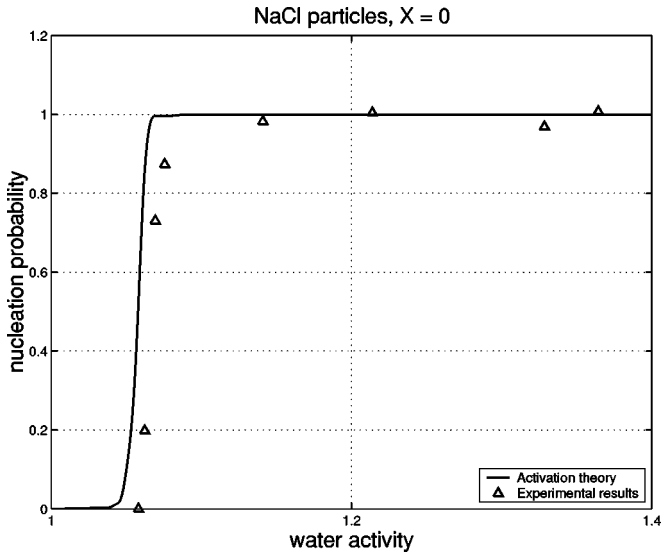

FIG. 13. Same as Fig. 11 but for *n*-propanol vapor mass fraction $X=0$.

nucleation of binary (*n*-propanol–water) vapor mixtures on insoluble (Ag) as well as on partially soluble (NaCl) particles has been investigated experimentally and theoretically at constant nucleation temperature.

While Ag is insoluble in both compounds considered, NaCl is soluble in water and insoluble in *n*-propanol. Correspondingly, for heterogeneous nucleation in unary water vapor the NaCl particles reveal a significantly smaller onset vapor phase activity as compared to Ag particles (see Fig. 4).

Surface changes of Ag particles caused by possible oxidation were surprisingly found not with facilitate the heterogeneous nucleation of the unary and binary vapors considered. A different behavior has been reported by Kotzick *et al.* [12] for carbon particles. A reaction with ozone lowered the critical water supersaturations for benzo[a]pyrene tagged carbon particles.

Heterogeneous nucleation probabilities have been measured as functions of the vapor phase activities and quantitatively compared with predictions by the Fletcher approach and/or the activation theory. The influence of the distribution of particle sizes on the nucleation probabilities has been accounted for in the model calculations. While the heterogeneous nucleation probabilities were found to approach zero below and one above certain onset vapor phase activities, an increase in the nucleation probabilities at a comparatively steep slope is observed around the onset activities.

The slopes of the nucleation probability versus vapor phase activity curves show an interesting behavior. For insoluble surfaces the theoretical slopes are generally found to be significantly steeper as compared to the experiment. The Fletcher approach shows somewhat stronger deviations as compared to the activation theory. The finite width of the particle size distribution was found to be insufficient to explain these differences. The results of this study seem to indicate a certain variability of surface properties of the nucleating particles leading to changes of the nucleation behavior. It is notable that the deviations of theoretical slopes from the experimental ones tend to be particularly pronounced for heterogeneous nucleation of unary vapors.

Particles soluble in the condensing liquid show a qualitatively different behavior. For heterogeneous nucleation of water-rich vapor mixtures on NaCl particles satisfactory agreement of the experimental slopes with model calculations according to the activation theory was found (see Figs. 11–13). This observation provides a strong indication that solution droplets with well defined surface are activated and no significant variability of the surface properties occurs. For increasing *n*-propanol vapor mass fractions the experimental slopes are found to be significantly smaller than the theoretical prediction, consistent with the above described behavior of insoluble particles. This is a clear experimental indication for a soluble-insoluble transition [26]. In the range of transition the calculations according to the activation theory were found to be very sensitive with respect to particle size.

For heterogeneous nucleation (activation) of soluble particles apparently a somewhat similar situation is encountered as for homogeneous nucleation in that experimental and theoretical slopes of the nucleation probability curves are found to be in good agreement. Furthermore, theoretical onset vapor activities agree fairly well with experiment for unary systems, while deviations occur for nucleation of binary vapors. For insoluble particles, however, the theoretical description of heterogeneous nucleation is considerably more complicated as compared to homogeneous nucleation because of the complex microscopic properties of the solid particle surfaces. Accordingly, deviations between theoretical and experimental slopes of the nucleation probability curves occur, and calculations of onset activities can lead to severe discrepancies even for unary systems, as discussed elsewhere [26].

For Ag as well as NaCl particles we have found that the curves describing the onset vapor activities for heterogeneous nucleation of binary vapor mixtures exhibit a convex shape (see Figs. 2 and 4). This indicates a comparatively weak mutual enhancement of heterogeneous nucleation of the two vapor compounds. It is interesting to note that a considerably more pronounced mutual enhancement has been observed for the case of homogeneous nucleation of *n*-propanol–water vapor [38].

While the Fletcher approach is restricted to heterogeneous nucleation on insoluble particles, the activation theory can be applied to soluble and partially soluble particles. The results of this study indicate that the activation theory is more successful than the Fletcher approach in predicting the slopes of the heterogeneous nucleation probabilities as well as onset vapor phase activities for the case of nucleation on the NaCl particles over the whole range of vapor mass fractions.

The activation theory is only applicable to particle surfaces with contact angle zero, i.e. fully wettable particles. Accordingly, our model calculations for heterogeneous nucleation on Ag particles are based on the Fletcher approach. Calculations using experimental values of the macroscopic contact angles [20] as well as calculations assuming contact angle zero have led to severe discrepancies. These and similar discrepancies between experimental data and theoretical calculations can probably be attributed to the choice of contact angles used in the calculations. We have achieved fairly good agreement between experimental results and model calculations for binary heterogeneous nucleation on Ag particles over the whole range of vapor mass fractions by using fit values of the contact angles, which are substantially lower than the macroscopic experimental values (see Fig. 3). For liquid *n*-propanol mass fraction zero, i.e., pure water, a fit contact angle of 35.6° was found reflecting the hydrophobic behavior of the Ag particles with respect to water. For increasing liquid *n*-propanol mass fractions the fit contact angle quite rapidly approaches zero, indicating complete wettability for *n*-propanol rich mixtures. The obtained fit contact angles may be considered as approximate values of microscopic contact angles, which refer to the microscopic properties of the particle surface.

The results of this study indicate that macroscopic surface properties, such as contact angles obtained from macroscopic measurements, will not be generally applicable for the

description of heterogeneous nucleation by nanoparticles. It is emphasized that the characterization of the microscopic properties of particle surfaces constitutes the key problem for a description of heterogeneous vapor nucleation. In turn heterogeneous nucleation experiments can provide information on the microscopic behavior of nanoparticle surfaces.

ACKNOWLEDGMENTS

This work was supported by the Austrian Science Foundation (Project No. 9421), by the Hochschuljubiläumsstiftung of the City of Vienna, and by the Academy of Finland (Projects Nos. 50623 and 173804).

[1] R.J. Charlson and T. Wigley, Sci. Am. **270** (2), 48 (1994).
[2] D.W. Dockery and C. Pope, Annu. Rev. Public Health **15**, 107 (1994).
[3] A. Laaksonen, V. Talanquer, and D.W. Oxtoby, Annu. Rev. Phys. Chem. **46**, 489 (1995).
[4] H. Arstila, K. Laasonen, and A. Laaksonen, J. Chem. Phys. **108**, 1031 (1998).
[5] I. Kusaka, Z.-G. Wang, and J.H. Seinfeld, J. Chem. Phys. **108**, 3416 (1998).
[6] J.H. Seinfeld and S.N. Pandis, *Atmospheric Chemistry and Physics: From Air Pollution to Climate Change* (Wiley, New York, 1998).
[7] P. Korhonen, M. Kulmala, and Y. Viisanen, J. Aerosol Sci. **28**, 901 (1997).
[8] S.L. Clegg, P. Brimblecombe, and A.S. Wexler, J. Phys. Chem. A **102**, 2137 (1998).
[9] N. Fletcher, J. Chem. Phys. **29**, 572 (1958).
[10] M. Lazaridis, M. Kulmala, and A. Laaksonen, J. Aerosol Sci. **22**, 823 (1991).
[11] R. Kotzick, U. Panne, and R. Niessner, J. Aerosol Sci. **28**, 725 (1997).
[12] R. Kotzick and R. Niessner, Atmos. Environ. **33**, 2669 (1999).
[13] C.C. Chen and C.J. Tao, J. Chem. Phys. **112**, 9967 (2000).
[14] C.C. Chen, C.C. Huang, and C.J. Tao, J. Colloid Interface Sci. **211**, 193 (1999).
[15] C.C. Chen, C.J. Tao, and H.J. Shu, J. Colloid Interface Sci. **224**, 11 (2000).
[16] S. Oatis, D. Imre, R. McGraw, and J. Xu, Geophys. Res. Lett. **25**, 4469 (1998).
[17] J. Han and S. Martin, J. Geophys. Res., [Atmos.] **104**, 3543 (1999).
[18] J. Porstendörfer, H.G. Scheibel, F.G. Pohl, O. Preining, G. Reischl, and P.E. Wagner, Aerosol. Sci. Technol. **4**, 65 (1985).
[19] E. Zapadinsky, B. Gorbunov, V. Voloshin, and M. Kulmala, J. Colloid Interface Sci. **166**, 286 (1994).
[20] R. Ortner, Master's thesis, University of Vienna, Vienna, Austria, 2000 (unpublished).
[21] D. Petersen, Ph.D. thesis, University of Vienna, Vienna, Austria, 2001 (unpublished).
[22] M. Kulmala, A. Lauri, H. Vehkamäki, A. Laaksonen, D. Petersen, and P.E. Wagner, J. Phys. Chem. B **105**, 11 800 (2001).
[23] L. Krämer, U. Pöschl, and R. Niessner, J. Aerosol Sci. **31**, 673 (2000).
[24] P. Wagner, J. Colloid Interface Sci. **105**, 456 (1985).
[25] T. Vesala, M. Kulmala, R. Rudolf, A. Vrtala, and P.E. Wagner, J. Aerosol Sci. **28**, 565 (1997).
[26] D. Petersen, R. Ortner, A. Vrtala, P.E. Wagner, M. Kulmala, and A. Laaksonen, Phys. Rev. Lett. **87**, 225703 (2001).
[27] A. Laaksonen, R. McGraw, and H. Vehkamäki, J. Chem. Phys. **111**, 2019 (1999).
[28] F.F. Abraham, *Homogeneous Nucleation Theory* (Academic Press, New York, 1974).
[29] D. Stauffer, J. Aerosol Sci. **7**, 319 (1976).
[30] M. Kulmala and A. Laaksonen, J. Chem. Phys. **93**, 696 (1990).
[31] A.W. Adamson, *Physical Chemistry of Surfaces*, 4th ed. (Wiley, New York, 1982).
[32] P. Hamill, R. Turco, C.S. Kiang, O.B. Toon, and R.C. Whitten, J. Aerosol Sci. **13**, 561 (1982).
[33] H. Köhler, Trans. Faraday Soc. **32**, 1152 (1936).
[34] A. Laaksonen, P. Korhonen, M. Kulmala, and R.J. Charlson, J. Atmos. Sci. **55**, 853 (1998).
[35] E. Vercher, M.P. Pena, and A. Martinez-Andreu, J. Chem. Eng. Data **41**, 66 (1996).
[36] R. Defay, I. Prigogine, and A. Bellemans, *Surface Tension and Adsorption* (Longmans, London, 1966).
[37] Y.S. Djikaev and D.J. Donaldson, J. Geophys. Res., [Atmos.] **104**, 14283 (1999).
[38] R. Strey, Y. Viisanen, and P.E. Wagner, J. Chem. Phys. **103**, 4333 (1995).
[39] Reaction times up to 120 s.
[40] It is a strongly hydrophobic substance.